

Northwestern University

Department of Biomedical Engineering

Digitally Adjustable Phrenic Nerve (DAPhNe) Stimulator

Final Report: Quarter II

PREPARED FOR

Matthew Glucksberg, M.S., Ph.D.
Professor of Biomedical Engineering, Northwestern University

Debra Weese-Mayer, M.D.
Chief, Center for Autonomic Medicine in Pediatrics, Lurie Children's Hospital

WRITTEN BY

Emma Cripe, Kirby Gong, Alexey Revinski, Michelle Wang
Northwestern University
16 March 2017

Executive Summary

Children with Congenital Central Hypoventilation Syndrome (CCHS) need advanced breathing support to improve their quality of life. While the current state-of-the-art device has sufficient functionality, it uses outdated technology and is far from ideal for use in small children. This report details the development of the implantable component of the Digitally Adjustable Phrenic Nerve (DAPhNe) Stimulator System and preliminary designs of the external component user interface. The technical feasibility of the system has been demonstrated with benchtop testing, and functional equivalence with the current Avery Breathing Pacemaker will be demonstrated through testing on a rabbit model.

The functions of the multi-setting wireless stimulator include:

- Phrenic nerve stimulation controlled externally by wirelessly communicated settings
- Wireless communication of data between the implant and the outside world
- Wireless power management

This report focuses on the development of the implant and details:

- Electrical and physiological considerations
- Implant system design
- Implant hardware implementation
- Implant software implementation
- Testing methods and results

This report also details the development of a user interface for the external device, as well as animal study preparations. Parts of this work include recommendations on future steps and strategies for demonstrating system reliability and feasibility of the functional prototype.

Table of Contents

Executive Summary.....	ii
Table of Contents.....	iii
Table of Figures.....	iv
1 Introduction	1
1.1 Avery Breathing Pacemaker	1
2 Implant Development.....	3
2.1 Overall System Model	3
2.2 Electrical and Physiological Considerations	4
2.2.1 Load Model	4
2.2.2 Stimulation Signal Requirements.....	4
2.2.3 Constant-Current Stimulation.....	4
2.2.4 Charge Balancing Considerations	5
2.2.5 Proposed Output Signal	9
2.3 Implant System Design	10
2.3.1 General Functional Interactions	10
2.3.2 Stimulation Circuit Model.....	11
2.3.3 Stimulation Circuit Model Rationale	12
2.4 Implant Hardware Implementation.....	13
2.4.1 Load.....	14
2.4.2 Electrode.....	14
2.4.3 Battery	15
2.4.4 Battery Charging Circuit.....	16
2.4.5 Wireless Charging Coil.....	17
2.4.6 Voltage Regulator: 3.3V	17
2.4.7 Polarity Switching Circuit	18
2.4.8 MCU Module	20
2.4.9 STIM Module.....	21
2.4.10 Near Field Communication Memory	22
2.4.11 Signal Acquisition Technology	23
2.5 Implant Software Implementation	24
2.5.1 Control Signals Model.....	24
2.5.2 Power Consumption Considerations in Microcontroller Software Design.....	26
2.5.3 Software Implementation	28
2.6 Reliability Considerations.....	32
2.6.1 Failure Mode Chart	32
2.6.2 Multiple Processors.....	32
2.6.3 Analog Error Detection.....	32
2.6.4 Backup Battery System.....	32
2.6.5 Full System Redundancy	33
2.6.6 Alert System.....	33
2.7 Testing	34
2.7.1 Power Consumption Testing	34
2.7.2 Device Output	36
2.7.3 Animal Testing.....	38
3 External Device Development	43
3.1 User Interface Development	43
3.1.1 User Interface Interviews.....	43
3.1.2 User Interface Design	44
4 Next Steps.....	48
4.1 Power Consumption Testing.....	48
4.2 Animal Testing.....	48
4.3 User Interface	48
4.4 Next Generation Prototype	48

Table of Figures

Figure 1: Mark IV Diaphragm Pacemaker from Avery Biomedical	2
Figure 2: Overall System Diagram	3
Figure 3: Monophasic and biphasic stimulation waveforms ²	6
Figure 4: Reactions at electrode/electrolyte interface ³	6
Figure 5: Capacitive Discharge Circuit and Pulse ⁴	7
Figure 6: Efficacy, safety, and electrode corrosion effects of various stimulation waveforms ⁶	8
Figure 7: Proposed stimulation signal	9
Figure 8: Implant prototype system diagram	10
Figure 9: Proposed stimulation circuit	11
Figure 10: (Left) Breakout Board Prototype; (Right) Dual PCB Prototype	13
Figure 11: Simulated Load.....	14
Figure 12: Modern stimulation electrode used by Mark IV system	14
Figure 13: LIR2450H coin cell battery (US quarter for comparison).....	15
Figure 14: Breadboard battery charging circuit	16
Figure 15: (Left) Wireless power transmitter and (Right) receiver	17
Figure 16: The modified LiPower board.....	18
Figure 17: A sample ADG1636 mounted on a breakout board.	19
Figure 18: STM8L-DISCOVERY Board from STMicroelectronics	20
Figure 19: The finished IPNS_v0.1_MCU module.....	20
Figure 20: The finished IPNS_v0.1_STIM module	21
Figure 21: ANT7-T-M24LR04E NFC Board from STMicroelectronics	22
Figure 22: nScope, plugged into a breadboard	23
Figure 23: Three microcontroller output control signals.	24
Figure 24: Signal Output: a) Breathing phases, b) Single pulse cycle, c) Logic control	28
Figure 25: Simulation over a 0.1s time period.....	34
Figure 26: Simulation over a single pulse	35
Figure 27: Output Signal: First Prototype	37
Figure 28: Output Signal: Second Prototype	37
Figure 29: Flow chart of experiment part 1 procedure	40
Figure 30: Flowchart of experiment part 2 procedure	41
Figure 31: User Interface Screens.....	47

1 Introduction

Children with Congenital Central Hypoventilation Syndrome (CCHS) need advanced breathing support to improve their quality of life. While the current state-of-the-art device has sufficient functionality, it uses outdated technology and does not support the needs of small children. This report documents progress made in the design of an implantable part of the Digitally Adjustable Phrenic Nerve (DAPhNe) Stimulator.

The functions of the DAPhNe Stimulator include:

- Phrenic nerve stimulation controlled externally by wirelessly communicated settings
- Wireless communication of data between the implant and the outside world
- Wireless power management

The DAPhNe Stimulator system consists of an external transmitter and an implant. This report details the development of the implant, as well as the design of the user interface for the external transmitter.

1.1 Avery Breathing Pacemaker

The existing gold standard in diaphragm pacing for CCHS patients is the Mark IV Diaphragm Pacemaker made by Avery Biomedical. It consists of an external transmitter box, about 2 lbs. in weight, which offers the doctor control over stimulation using a series of knobs and screws, seen in Figure 1. The external transmitter sends inductive pulse waves through tissue to the implant; circuitry of the implant conditions the signal to output nerve stimulation pulses. This design, although functional and extremely reliable, is unintuitive, cumbersome (especially for children), offers the patient only one pre-set setting, and is not waterproof. The team hopes to improve upon some of these deficiencies with the DAPhNe Stimulator.



Figure 1: Mark IV Diaphragm Pacemaker from Avery Biomedical

As seen in Figure 1, the adjustment interface consists of unitless knobs that are there just for blind adjustment. Doctors have to use extensive monitoring equipment when adjusting these devices. Another problem with this interface is that it is accessible to the patient, and can be accidentally modified, possibly resulting in injury to the patient. Also, because the patient is tethered to the device, ability to perform water activities is virtually non-existent when the device is in use.

The novel DAPhNe Stimulator System aims to provide CCHS patients with a greater range of ventilatory support, greater mobility, and ability to perform water activities.

This work reports on system design and reliability considerations for the device; testing methods and results; design of a proof-of-concept animal study; and recommendations on future device development.

For any abbreviations used in this report, please refer to Appendix A.

2 Implant Development

2.1 Overall System Model

Figure 2 shows the overall system model. The system consists of two devices - an implantable phrenic nerve stimulator, and an external control module. The external component will have a digital interface for the patients and their doctors, giving complete control over the patient's breathing settings to the doctor, and extended control over his or her breathing modes to the patient. The transmitter will be used to communicate with and charge the implant wirelessly.

The scope of this project primarily includes the development of the implant, with some preliminary development of the external device's user interface.

The implant's main feature is an ultra-low-power microcontroller and a stimulation circuit controlled by it. The two circuits have their own power supplies that are powered by a 3.7V Li-Ion battery. Receivers for data and power communications are included in the circuit. The casing of the implant will be made of titanium and will act as the "body ground" reference potential. The stimulation electrode will be driven high and low with respect to the device case potential.

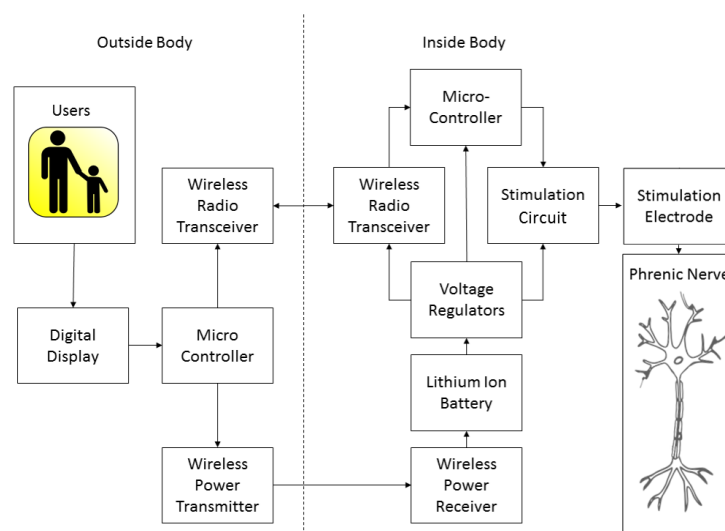


Figure 2: Overall System Diagram

2.2 Electrical and Physiological Considerations

2.2.1 Load Model

The phrenic nerve and surrounding tissue, as the final target of the implant circuit, is modeled in our testing and simulations as a $1k\Omega$ resistor in parallel with a $10nF$ capacitor, based on recommendation from Avery Biomedical.

2.2.2 Stimulation Signal Requirements

As per information obtained from our client, Dr. Debra Weese-Mayer, M.D., and current literature on the subject, the optimal stimulation parameters have been gathered in Table 1.

Table 1: Required Stimulation Pulse Parameters

	Pulse Frequency	Pulse Width	Pulse Amplitude	Breaths Per Minute	Inspiration Time
Values	8-20 Hz	150-200 μs	0 - 9.9 mA	10 - 30 bpm	1.0 - 1.2 ms

2.2.3 Constant-Current Stimulation

Nerve-stimulating devices use various control circuits to manage the charge injected into the nerve tissue. The two most utilized types are Constant Voltage Stimulation (CVS) or Voltage Controlled Stimulation, and Constant Current Stimulation (CCS), or Current Controlled Stimulation. In the former, a steady voltage is applied across the tissue load for a certain period of time, and current that passes through the tissue highly depends on the impedance of the load. Hence, CVS circuits have little control over the charge that they pass through the load. However, some control can be achieved with a current/impedance sensing feedback.

Constant Current Stimulation circuits force a constant current flow through the tissue, no matter the tissue impedance. While this passes the same stimulating current through the nerve-surrounding tissue no matter the load and, thus, results in more effective stimulation, these devices

need to have high compliance voltage in order to be able to force the desired current through an unexpectedly high load impedance. CCS simulation has also been shown to be less energy efficient than CVS.¹

Because the proposed device is a *rechargeable* life-sustaining nerve stimulator requiring reliable “self-adjusting” charge control, a constant-current stimulation circuit was developed.

2.2.4 Charge Balancing Considerations

The nerve has to be stimulated cathodically - meaning, the surrounding tissue voltage potential needs to be brought down closer to the negative internal cell membrane potential in order to depolarize the nerve and cause downstream diaphragm contraction. This is achieved by driving a monopolar electrode partially encompassing the nerve below the body ground reference. Current, then, flows from the device case to the stimulation electrode.

Stimulation by single negative pulses is called monophasic - having one negative pulse phase (Figure 3.a). This is easily implemented in hardware, and is great for short-term nerve stimulation in some applications. However, over a long period of time, this type of stimulation can damage the nerve and raise electrode impedance significantly, overburdening the stimulating circuitry of the device.²

¹ Ghovanloo, M. "Switched-capacitor based implantable low-power wireless microstimulating systems." *2006 IEEE International Symposium on Circuits and Systems*. doi:10.1109/iscas.2006.1693055.

² Merrill, Daniel R., Marom Bikson, and John G.r. Jefferys. "Electrical stimulation of excitable tissue: design of efficacious and safe protocols." *Journal of Neuroscience Methods* 141, no. 2 (2005): 171-98. doi:10.1016/j.jneumeth.2004.10.020.

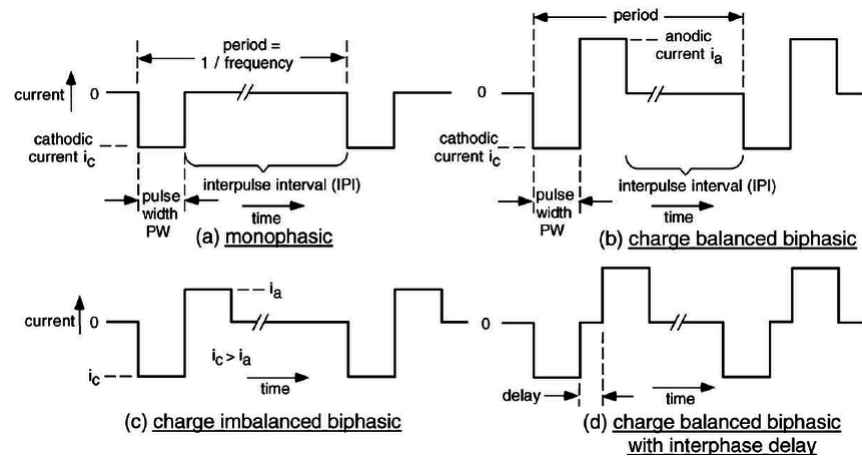


Figure 3: Monophasic and biphasic stimulation waveforms²

These changes are due to the fact that in the tissue area immediately surrounding the electrode, charge flows in the form of ions, but in the stimulation circuit, charge flows by electron displacement. As the charge crosses the electrode/electrolyte interface, there are Faradaic (charge transferring) chemical reactions taking place - metallic ions become metal atoms, and vice versa (Figure 4). Corrosion of the electrode surface raises the electrode impedance (and, hence, perceived load impedance), and accumulation of metallic ions in the tissue can cause nerve damage over time. If the passed charge is not balanced correctly, some irreversible chemical reactions can cause permanent disruption of the nerve function.³

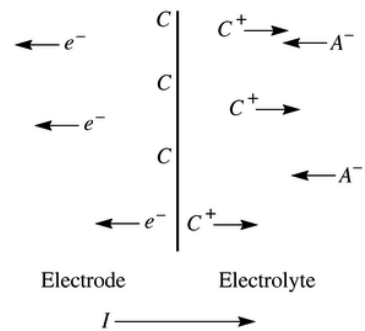


Figure 4: Reactions at electrode/electrolyte interface³

³ Webster, John G., and John W. Clark. *Medical instrumentation: application and design*. 4th ed. Hoboken, NJ: John Wiley & Sons, 2010.

There are two ways to fix this. First, some devices (including Avery's Mark IV - our model device) use capacitor-based stimulation circuits, a simple example of which is shown in Figure 5. A capacitor is charged up to a certain voltage, then discharged into the tissue via an electric switch, and charged up again. This way, charge that passes through tissue in one direction during each pulse flows in reverse as the capacitor charges up again.⁴

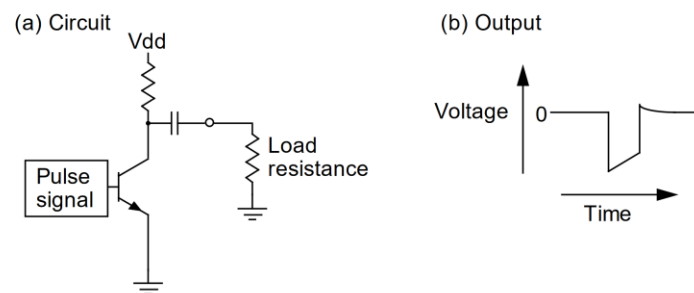


Figure 5: Capacitive Discharge Circuit and Pulse⁴

However no such auto-recharge method can be utilized in a constant-current stimulation circuit (unless it is a hybrid switched capacitor circuit) because the current through the tissue is directly controlled by a programmable current sink.

Biphasic stimulation accomplishes charge balancing by using a current source and a current sink connected to a dual power supply to drive stimulation electrode high or low with respect to body ground, achieving a waveform seen in Figure 3.b and Figure 6.b. While accomplishing charge balancing, it has been shown to damage nerve tissue.⁵

⁴ Webster, John G. *Design of cardiac pacemakers*. New York: Institute of Electrical and Electronics Engineers, 1995.

⁵ Merrill, Daniel R., Marom Bikson, and John G.r. Jefferys. "Electrical stimulation of excitable tissue: design of efficacious and safe protocols." *Journal of Neuroscience Methods* 141, no. 2 (2005): 171-98. doi:10.1016/j.jneumeth.2004.10.020.

There is another way to balance the charge without damaging the tissue or causing significant electrode problems. The method is called “charge-balanced biphasic stimulation with slow reversal”, as per work by Merrill, et al.⁶ The waveform is shown in Figure 6.f.

This waveform allows charge balancing to occur over a long time, imitating a nice recharge waveform seen in switched-capacitor circuits, avoiding instantaneous damage to the tissue seen in b) or e) and inducing minimal corrosion to the electrode. In this application, tissue damage is unacceptable; the longevity of the stimulation requires the stimulation electrode to be able to pass charge for years. Out of all of the stimulation waveforms and their tradeoffs presented in Figure 6, the charge balanced biphasic waveform with slow reversal (Figure 6.f) offers the best traits fitting the application.

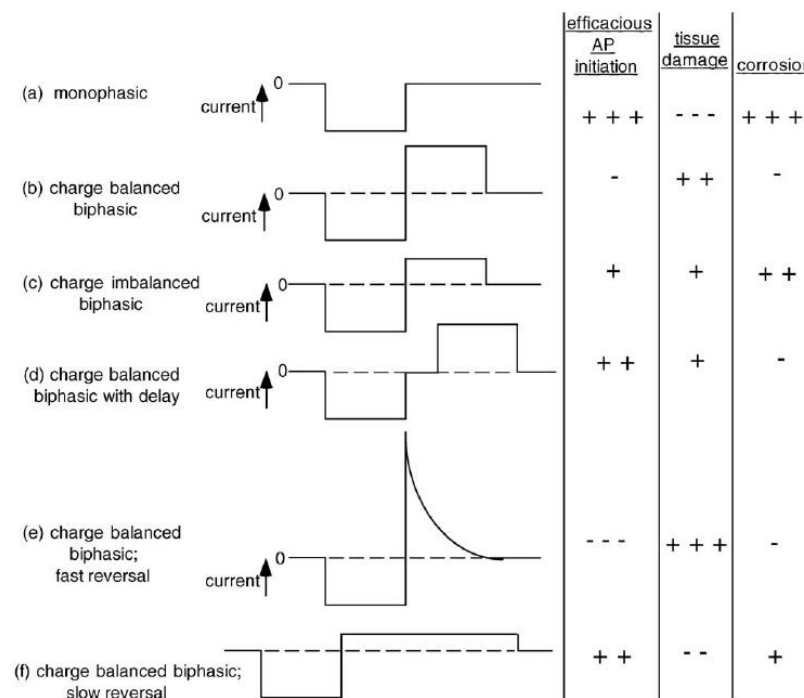


Figure 6: Efficacy, safety, and electrode corrosion effects of various stimulation waveforms⁶

⁶ Merrill, Daniel R., Marom Bikson, and John G.r. Jefferys. "Electrical stimulation of excitable tissue: design of efficacious and safe protocols." *Journal of Neuroscience Methods* 141, no. 2 (2005): 171-98. doi:10.1016/j.jneumeth.2004.10.020.

2.2.5 Proposed Output Signal

Following Figure 6.f, the optimal simulation signal in this application has been modeled as seen in Figure 7. V_C is current control signal voltage; R_L is current control resistance, and D is a ratio constant. The output signal consists of one large but short negative pulse, followed by a small positive pulse over a longer time period. To balance the charge correctly, each pulse needs to pass the same amount of charge through the tissue. This means that the area under each pulse (current x time = charge) needs to amount to the same value for both negative and positive pulses. A factor of 10 was chosen for ease of implementation and testing; hence, the recharge pulse is 10 times smaller in amplitude and 10 times longer in duration than the negative stimulation pulse.

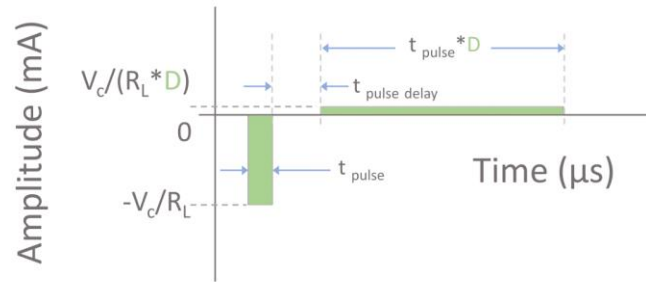


Figure 7: Proposed stimulation signal

2.3 Implant System Design

Figure 8 shows the circuit model for the implantable device. Reliability and redundancy considerations are yet to be incorporated into this particular model; however, this model was used to make the team's first two system prototypes.

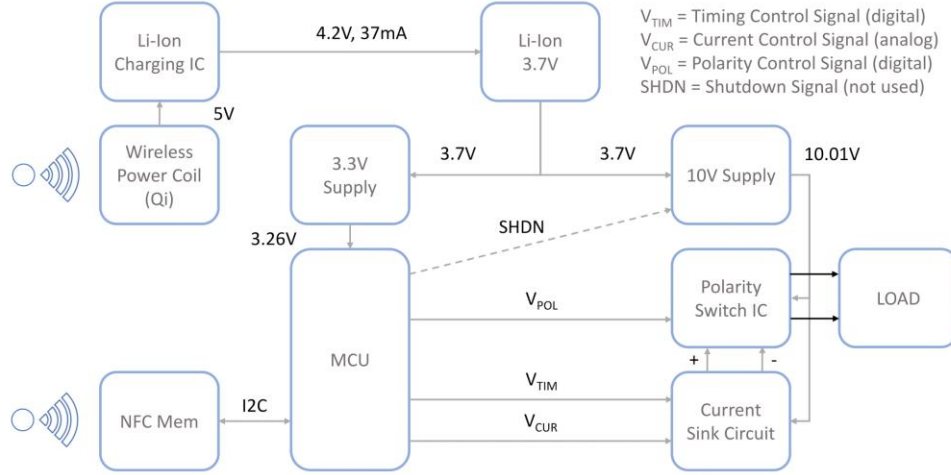


Figure 8: Implant prototype system diagram

2.3.1 General Functional Interactions

Ideally, the implant will be powered by a 3.7V medical grade lithium polymer battery. However, for the purposes of prototyping, the system uses a large coin cell 3.7V Li-Ion battery. The battery provides power to two voltage sources; the 3.3V buck-boost converter circuit supplies the microcontroller (MCU) and supporting circuitry with a steady 3.3V no matter the battery voltage (3.0-4.2V), while the 10V boost converter supplies the stimulation circuit. This high voltage is needed to be able to pass enough current through the model load. The MCU controls the stimulation circuit with three signals (explained in Section 2.5.1), and communicates with a wireless NFC tag. The battery is charged with a specialized Li-Ion battery management component, which is powered wirelessly via an inductive power coil.

2.3.2 Stimulation Circuit Model

Figure 9 shows a circuit diagram of the proposed stimulation circuit. It is controlled by the microcontroller using three signals discussed in the Section 2.5. Current is controlled by a programmable constant-current sink, implemented with a precision op-amp, a low R_{dson} MOSFET, and a high-precision 200 Ohm resistor. The current flows from the +10V source to device ground through the load connected to a dual SPDT switch (S1), Q2, and R2. Negative feedback of the op-amp circuit forces the voltage seen at the non-inverting input to be applied across the 200 Ohm resistor, thus controlling current flowing through the load. A timing signal lets Q1 conduct the pulse amplitude signal and, hence, control the current sink feedback. With R2 value of 200 Ohms, 1V at V_{DAC} equates to 5mA of current passed through the load. Assuming ideal Q2 and SPDT switch (no resistance), the maximum range of the amplitude control signal required is 0-1.67V for 0-8.3mA current pulses. Higher compliance voltage ($>10\text{V}$) is needed in order to pass higher current through the load. See Appendix B for a detailed analysis of the circuit.

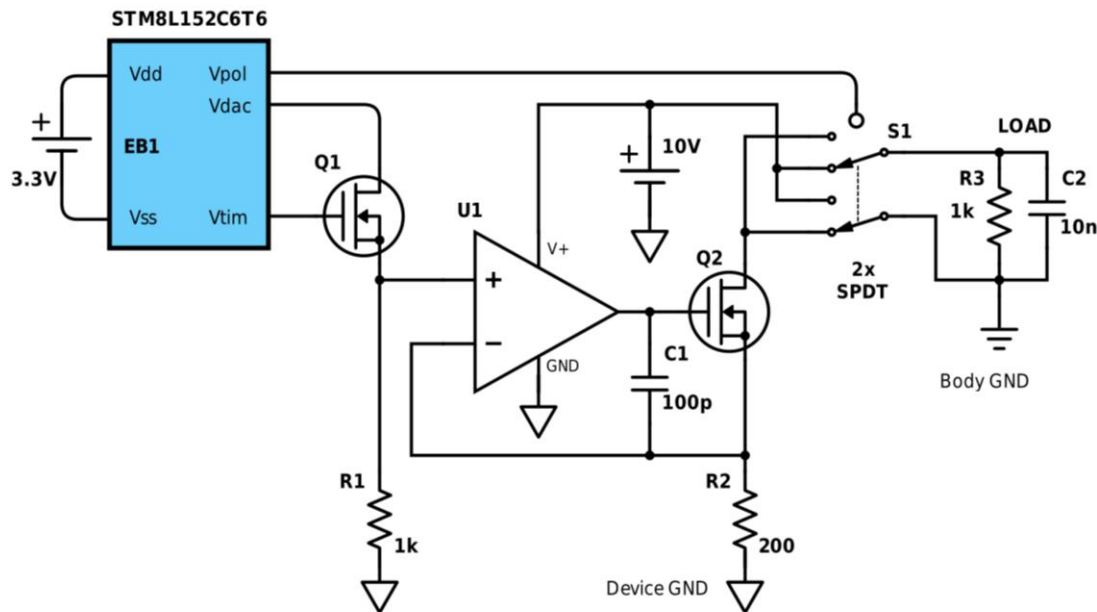


Figure 9: Proposed stimulation circuit

2.3.3 Stimulation Circuit Model Rationale

Because the system needs to output negative *and* positive stimulation pulses, the circuit would ideally utilize a dual supply (more than $\pm 12\text{V}$, or 24V difference in potential). A current source and sink would be turned on individually to pull the current up or down relative to a middle node.

However, the battery voltage is planned to be 3.7V; achieving a 24V potential difference using this starting voltage would be very inefficient, and a current sink/source circuit would double the number of components needed for current control - this is neither power nor component/space efficient. The proposed circuit solves this by using just a single +10V supply, which will provide enough compliance voltage for most stimulation scenarios.

The current only flows from the +10V node into the current sink across the load. However, the body ground and stimulation electrode are connected and disconnected to appropriate electrical nodes by a dual SPDT switch shown in Figure 9. During negative pulses, the switches are turned on, and the body ground is connected to the +10V source output; the electrode is connected to the current sink node. This way, the electrode remains negative with respect to body ground during the pulse, and this achieves cathodic stimulation. After the negative pulse, the switches are turned off, and body ground is connected to the current sink; the stimulation electrode gets connected to the +10V source output. During this next pulse, the electrode remains positive with respect to body ground, and a positive recharge pulse is achieved. As mentioned before, “body ground” in this application is the device’s titanium case, and thus the monopolar electrode is driven high and low with respect to the device’s case using only a single 10V supply and a single current sink circuit, which saves both PCB space and lowers power dissipation by extra components.

2.4 Implant Hardware Implementation

The team developed two prototypes of the implantable stimulator. The first prototype of the system was created using off-the-shelf boards, breakout boards for individual small components, and generic passive components. Some of these components were still used in the second prototype, but a lot of them were “locked” into two PCB modules that constitute the current prototype of the system. Figure 10 shows both prototypes. The following sections discuss the design of the second prototype, with some references to the first. Refer to Appendix C to see how each of the following components fits into the system. Additionally, see Appendix D for the Bill of Materials.

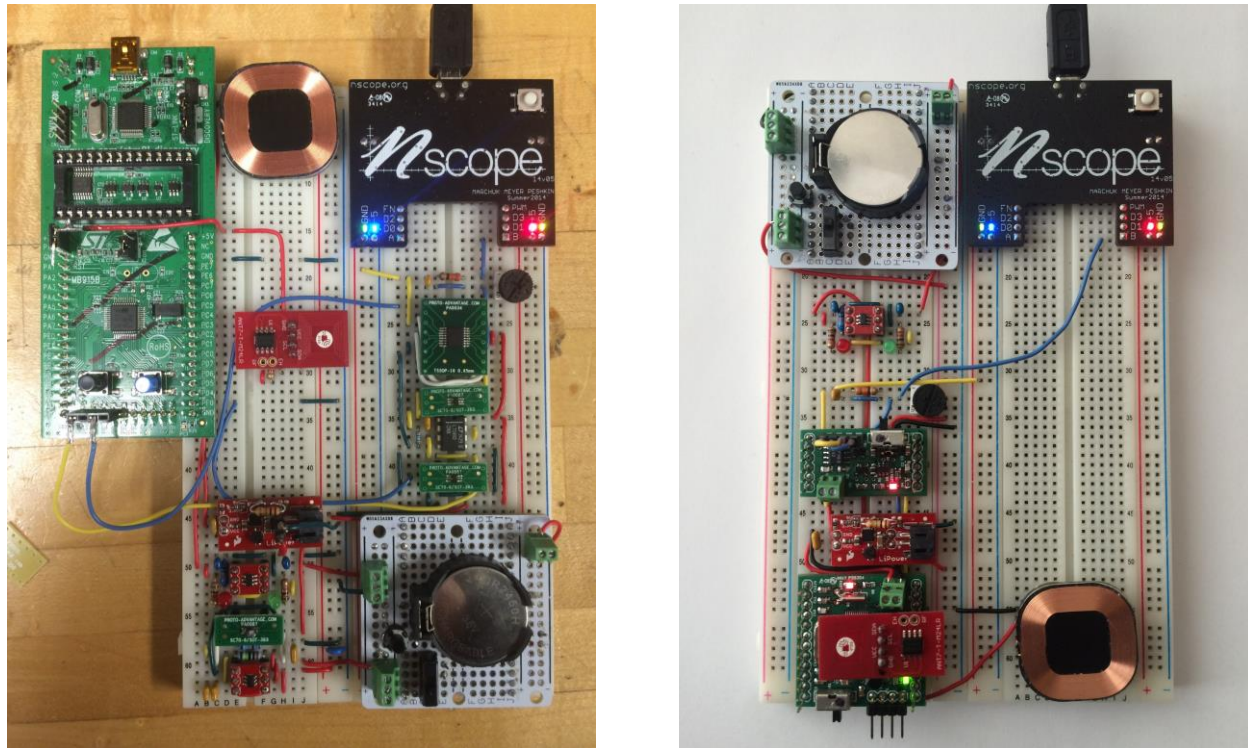


Figure 10: (Left) Breakout Board Prototype; (Right) Dual PCB Prototype

2.4.1 Load

As mentioned previously, the phrenic nerve was approximated with a $1\text{k}\Omega$ resistor in parallel with a $1\mu\text{F}$ capacitor, as is used by Avery in their documentation and development. The resistance was simulated using a 330Ω resistor in series with a $1\text{k}\Omega$ knob potentiometer for adjustability. The load in the current prototype can be seen in Figure 11.



Figure 11: Simulated Load

2.4.2 Electrode

The most current prototype has a screw-in port specifically designed to interface with a modified version of the stimulation electrode currently used by Avery, seen in Figure 12. This will allow for some backward compatibility with the Mark IV transmitter. Patients using Avery's Mark IV who may want to switch to the DAPhNe System will not have to undergo electrode placement surgery again (unless medically necessary). In addition, this allows for a better experimental control between the DAPhNe Stimulator and Avery's device during testing, as the same electrode can be used with both devices in a comparison study.

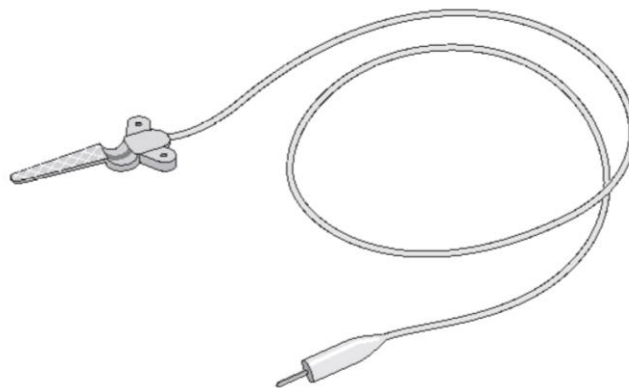


Figure 12: Modern stimulation electrode used by Mark IV system

2.4.3 Battery

The LIR2450H battery, seen in Figure 13, was used in both prototypes. It is a rechargeable lithium-ion coin cell battery manufactured by Tenenergy. It is 24.5mm in diameter and 5mm in height, with a nominal voltage of 3.6V, and capacity of about 190mAh. See Appendix E for a summary of the datasheet. This battery is sufficient for development and charging purposes, and has the desired chemistry that will be used in the actual implant a “lithium polymer” build version will be used. Future iterations will need to utilize batteries that have larger capacities, better energy densities, and built-in overvoltage protection circuits.



Figure 13: LIR2450H coin cell battery (US quarter for comparison)

2.4.4 Battery Charging Circuit

In order to charge the battery properly, a specialized battery charging circuit are required. Lithium ion chemistry batteries are charged using Constant Current/Constant Voltage (CC/CV) charge profiles. As the names imply, faster charging begins using a steady, low (relative to full capacity) constant current through the battery. As the battery recharges, its output voltage will rise, and at about 4.2V the battery charging circuit switches to constant voltage mode, which puts a constant 4.2V across the battery terminals until the current draw across the battery becomes minimal, indicating that it is full. The battery charging circuit, Figure 14, uses the MCP73831T-2ACI charging chip from Microchip, which is designed specifically for lithium ion batteries; it takes in a 5V input from the wireless charging coil and performs all the aforementioned functions. During charging the circuit shown in Figure 14 lights up a red LED, and once charging is completed, the green LED is powered. For more detail on the design of the battery charging circuit please see Appendix F.

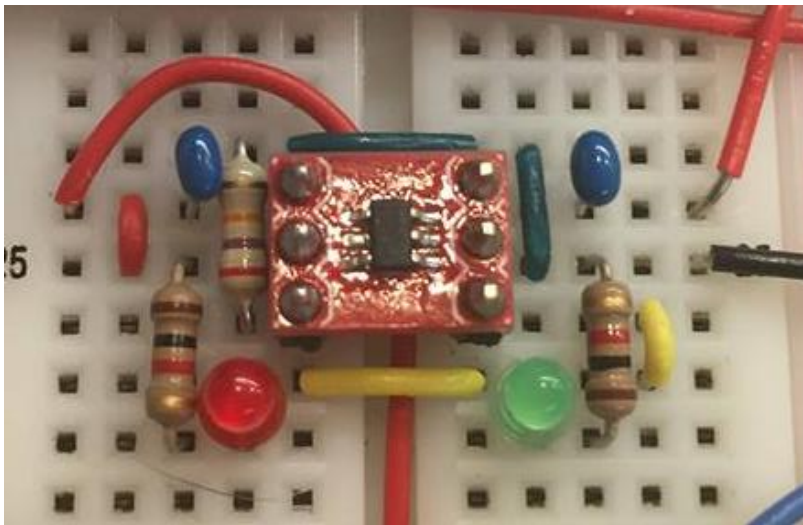


Figure 14: Breadboard battery charging circuit

2.4.5 Wireless Charging Coil

Feeding into the battery charging circuit is a steady 5V source, which must be able to provide at least 50mA for the current design (the maximum instantaneous current draw of the circuit, including battery charging). This is accomplished by using the STEVAL-ISB039V1 evaluation tool set for the STM32F0 and STWLC03 chips – power transmitter and receiver, respectively (Figure 15). This system uses 1W Qi protocol, see Figure 15. When the coils are aligned and close together, power is wirelessly transmitted to the receiver coil, which then output a steady 5V. The evaluation board can also be programmed to act as a simplified CC/CV lithium ion battery charger using I²C, but this functionality was not used. In addition, the board is capable of detecting when power transfer is successfully taking place and when there is interference in communication; this will be very useful in the development of the external transmitter.

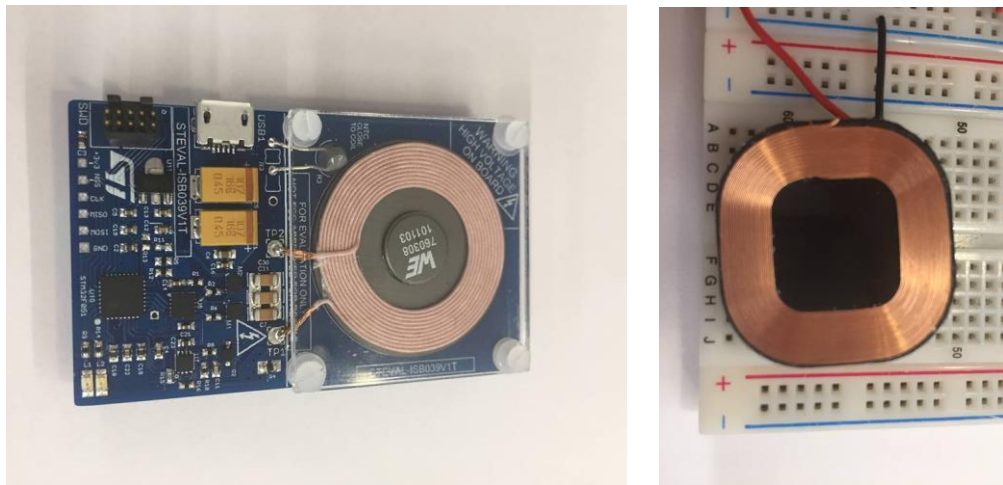


Figure 15: (Left) Wireless power transmitter and (Right) receiver

2.4.6 Voltage Regulator: 3.3V

The microcontroller runs most efficiently on a 3.3V power supply. However, the battery voltage decreases over time – the battery starts out at about 4.2V fully charged, and decreases to about 3.0 volts at critically low capacity. So, the battery voltage must be regulated with an output of a steady

3.3V. For this, the team used an off-the-shelf voltage regulator from SparkFun Electronics, based on the TPS61200, a low-power buck-boost converter chip from Texas Instruments. The board, called LiPower (Figure 16), is configured to run off of a lithium ion battery, with selectable voltage outputs of 3.3V or 5V, overtemperature protection, and an undervoltage lockout (UVLO) feature. The UVLO capability is essential for the longevity of battery life; it locks the boost converter from drawing any more current once the battery voltage reaches a certain low limit. This prevents overdraining the rechargeable battery. The default UVLO threshold was 2.75V, but by soldering an additional $1\text{M}\Omega$ resistor in parallel with one of the board resistors, the UVLO threshold was adjusted to 3.0V, as the LIR2450H battery requires. For more information regarding the UVLO modification, and testing of the LiPower module, see Appendix G.

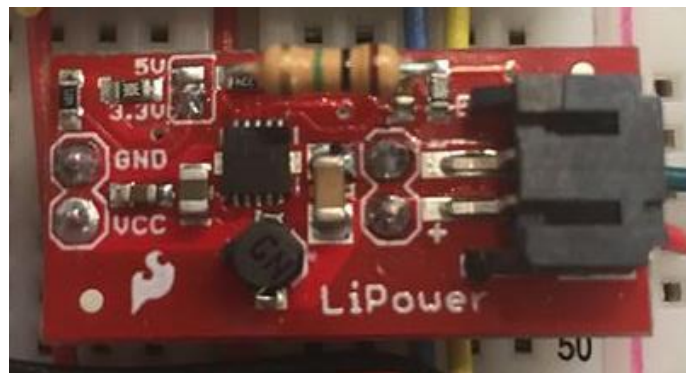


Figure 16: The modified LiPower board

2.4.7 Polarity Switching Circuit

Polarity switching circuit was implemented in the first breakout board prototype, and successfully modified stimulation signal, but has not yet been incorporated into the dual PCB prototype due to an electrical fault found in the design of the circuit. The original prototype used a 10V-rated low power dual analog SPDT switch from Analog Devices, model ADG1636 (Figure 17). While the correct signal output was collected, the team did not consider overvoltage protection of the inputs

of the chip. The problem is that if the power to the chip is off but there are positive potential signals at the device's inputs, those signals find their way into the power line, which, in turn kept damaging the powered-off 10V boost converter. Possible solutions have been postulated, but not yet tested. A solution may be purely hardware - using clamping diodes so that current cannot flow back into the power line, or it may involve software fixes like pulling down all inputs to the switch IC when the power to it is off. These will be implemented in a future prototype. For more detail on the nature of the error, and possible solutions, see Appendix H.

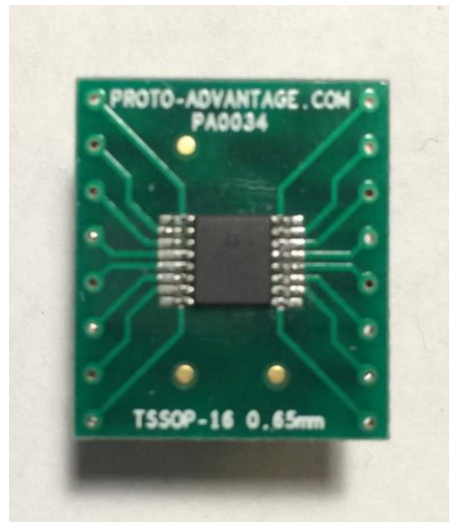


Figure 17: A sample ADG1636 mounted on a breakout board.

2.4.8 MCU Module

The microcontroller family of choice is the STM8L152 series of the ultra-low-power 8-bit microcontrollers from STMicroelectronics. The specific microcontroller in the current prototype is the STM8L152C6T6, with 32 kB Flash, 2 kB RAM, and 1 kB EEPROM. It offers power consumption values down to $\sim 0.4\mu\text{A}$ in the lowest power setting at body temperature, and has a footprint of only 9mm x 9mm. This version of the STM8L152 microcontroller is the family standard used in the STM8L-DISCOVERY evaluation board (Figure 18). This evaluation board was used in the first implant prototype, and the STM8L152C6T6 MCU was kept in the second prototype design for the sake of hardware and software compatibility with previous development work. A PCB prototype was developed for this microcontroller, seen in Figure 19. Refer to Appendix I for detailed design information about the designed MCU module.



Figure 18: STM8L-DISCOVERY Board from STMicroelectronics

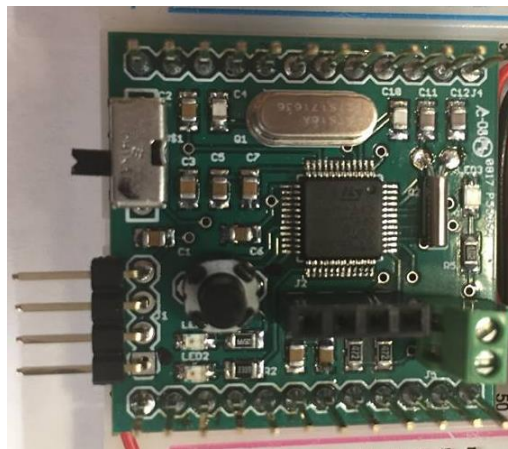


Figure 19: The finished IPNS_v0.1_MCU module

STM8L152C6T6, however, has the largest footprint among its family peers, and the STM8L family offers a lot of other microcontrollers that have less features, smaller footprint, and lower power consumption; one of these microcontrollers may be chosen later in the development process as a replacement for STM8L152C6. The microcontroller's software package is stored in an Open Source Design Repository described in Appendix J and is discussed in Section 2.5 below.

2.4.9 STIM Module

Most of the stimulation circuitry – with the exception of the polarity switch circuit – has been verified and tested for component compatibility and correct output. This allowed for creation of a unified PCB module containing all of the stimulation-related components seen in the Proposed Stimulation Circuit diagram in Figure 9, not including the microcontroller and the polarity switch circuit. Refer to Appendix K for detailed description of the design. The stimulation circuit PCB module can be seen in Figure 20.

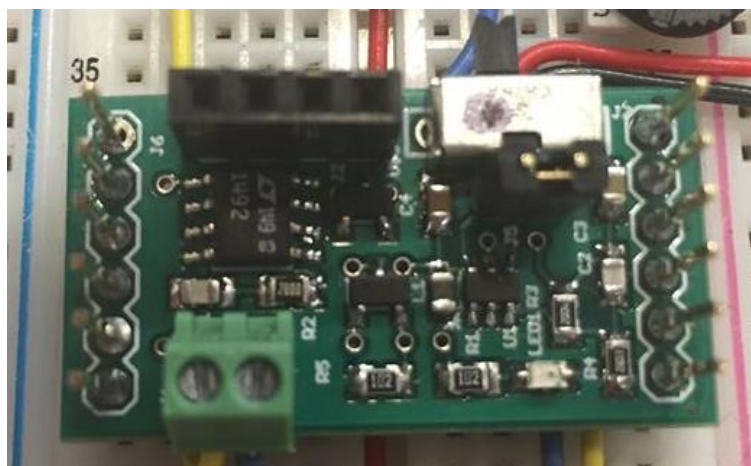


Figure 20: The finished IPNS_v0.1_STIM module

2.4.10 Near Field Communication Memory

As mentioned in previous reports, the wireless technology for this application was chosen to be Near-Field Communications (NFC) technology. It provides the physical security of close-range communications and software security features such as device passwords, identification features, and others. It can be combined with a magnetic reed switch to provide even better security - programming would only take place if a magnet is placed nearby. NFC technology is utilized in wireless card and

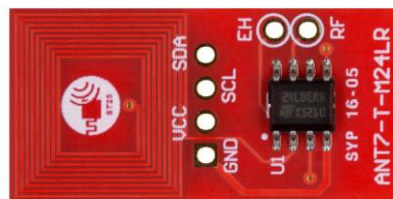


Figure 21: ANT7-T-M24LR04E NFC Board from STMicroelectronics

key readers, some mobile phone applications, and other short-range applications. Because two way communication only requires an external reader and a passive “tag” as part of the implant, this technology would be a much more power-conscious choice for this application than some other short-range technologies. Combined with the mentioned magnetic reed switch feature, this technology is sure to provide the most secure, reliable, and power-conscious solution available to the patient at this time. The current prototype uses a reference board from STMicroelectronics that uses their M24LR04 NFC memory IC and a 14mm x 14mm antenna for effective communication (Figure 21). The board directly plugs into the microcontroller module. The board design will need to be incorporated into further prototype iterations as part of the main printed circuit.

2.4.11 Signal Acquisition Technology

For testing purposes, it was important to be able to observe the voltage across the load. This was done using a breadboard-compatible oscilloscope system designed by the Northwestern University faculty, called nScope. The chip can be seen in Figure 22. nScope is capable of capturing signals $\pm 5V$ in amplitude at frequencies up in the MHz range. Its resolution and capabilities, as well as portability and compatibility with a PC system, makes it perfect for demo and testing uses.



Figure 22: nScope, plugged into a breadboard

2.5 Implant Software Implementation

2.5.1 Control Signals Model

In order to achieve the output signal shown in Figure 7, the circuit must control the timing, current amplitude, and polarity of the stimulation pulses. Hence, three control signals are required. They are shown in Figure 23.

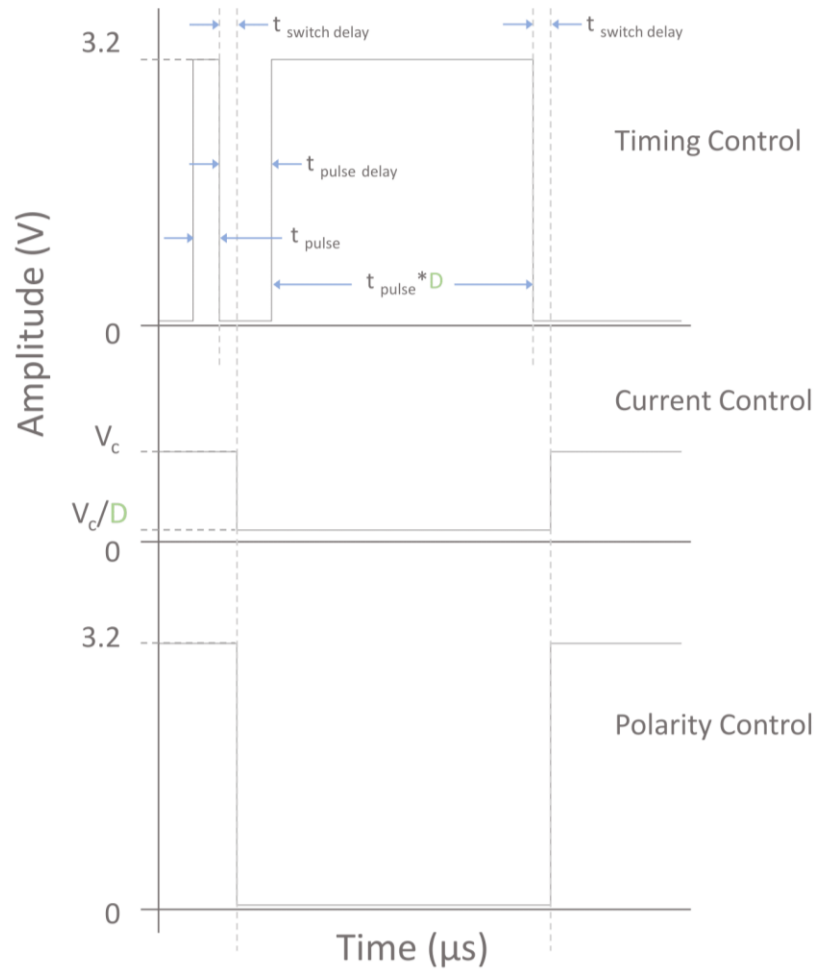


Figure 23: Three microcontroller output control signals.

In relation to the circuit in Figure 9, the three control signals correspond to the three signals coming from the microcontroller: V_{TIM} is Timing Control, V_{DAC} is Current Control, and V_{POL} is Polarity Control. All three signals direct outputs from the MCU. Timing and polarity control signals are digital and use digital timer outputs, while the current amplitude signal is an analog voltage; it utilizes the microcontroller's built-in analog-to-digital converter (ADC) unit.

A careful eye will notice that as opposed to Figure 6.f the positive pulse in the proposed output signal comes after the negative pulse after a certain delay. This delay was incorporated in order for the analog signal coming from the microcontroller to stabilize at a lower level, which takes some time because digital-to-analog converters employ capacitors, and hence cannot switch to a new level instantaneously. The delay also allows for the polarity switching circuit to stabilize and connect appropriate nodes to each other as well. It has been shown that a small delay does not affect nerve function and is just as effective as the signal shown in Figure 6.f.⁷ In fact, experiments on auditory nerves have shown that longer interphase delays resulted in smaller simulation thresholds for the next pulse.⁸ So the inter-pulse delay in the proposed signal may help the efficacy of simulation.

⁷ Davidovics, Natan S., Gene Y. Fridman, Bryce Chiang, and Charles C Della Santina. "Effects of Biphasic Current Pulse Frequency, Amplitude, Duration, and Interphase Gap on Eye Movement Responses to Prosthetic Electrical Stimulation of the Vestibular Nerve." *IEEE Transactions on Neural Systems and Rehabilitation Engineering* 19, no. 1 (2011): 84-94. doi:10.1109/tnsre.2010.2065241.

⁸ Prado-Guitierrez, Pavel, Leonie M. Fewster, John M. Heasman, Colette M. McKay, and Robert K. Shepherd. "Effect of interphase gap and pulse duration on electrically evoked potentials is correlated with auditory nerve survival." *Hearing Research* 215, no. 1-2 (2006): 47-55. doi:10.1016/j.heares.2006.03.006.

2.5.2 Power Consumption Considerations in Microcontroller Software Design

Recent advances in microcontroller technology brought to the market devices that can achieve current consumption values down to a couple of microamperes. However, even these devices can consume a lot of power. The following considerations were taken into account when designing the software of the system.

The central processing unit (CPU) of any microcontroller is by far the largest power consumer in the system. For instance, in our chosen STM8L152 devices, CPUs can consume ~2mA on average at body temperature (see Appendix J for link to datasheet) at highest settings. Thus, the CPU should be on for as little time as possible and be shut-off or in the lowest power mode available for the rest of the time.

Microcomputing systems have to be clocked (pulsed) at high frequencies in order to perform discrete calculation steps. The speed at which the device is clocked is proportional to power consumption. The higher the clocking speed, the higher the power dissipation. Hence, for the majority of the device program cycle, the MCU needs to utilize the smallest frequency possible. However, there is a tradeoff between low clocking frequency and having the device on for the shortest time. For instance, at higher clocking frequencies, the CPU can perform its functions much faster and thus consume some current over a very short amount of time. Low frequencies can result in smaller power consumption per unit time, but the CPU would be on for longer, and hence, will consume smaller current over a longer period of time, which may come out to be a larger consumption overall.

The microcontroller in the DAPhNe Stimulator also has various useful peripherals, most of which are not utilized in the application. Peripherals, just like the CPU, need to be clocked in order to

operate. Hence, it is important to gate the unused peripherals so they do not consume unnecessary power.

The largest-current-consuming peripherals are those that deal with analog voltages, as they employ complicated capacitor switching circuits, as opposed to simple digital switches. To prove the point, as per the STM8L152 datasheet, the analog-to-digital converter (ADC) and digital-to-analog converter (DAC) consume up to 1500 μ A and 370 μ A, respectively, regardless of clock frequency (see Appendix J for link to datasheet). Hence, even on lowest device settings, these would consume 0.3-1.5mA each if kept on. Thus, they need to be shut-off for as long as possible during the cyclical operation of the program.

Every microcontroller has general input/output pins that can be programmed to be connected to some internal circuitry. Input pins that accept current from a defined logic level (low or high) need to be configured in either “pull-up” or “pull-down” mode depending on the state; in case of a high impedance input, the pin needs a “floating” configuration in order to minimize waste of current. Otherwise, even slight static disturbances can cause significant current consumption over time.

Likewise, for output pins, a “push-pull” configuration is needed if the pin is driving a low-impedance load, and an “open-drain” configuration is needed if the pin is interfaced with a high impedance load (most communication systems) or is not connected to any defined state.

Finally, the amount of instructions employed in the program needs to be as low as possible to minimize the amount of time the device is in a high power computing mode.

2.5.3 Software Implementation

Physiologically, the device needs to have two basic states - an inspiration state, when the MCU is actively stimulating the phrenic nerve, and an expiration state, when the device is silent (Figure 24.a). Intuitively, the device needs to be “shut-off” during the expiration state, conserving as much power as possible.

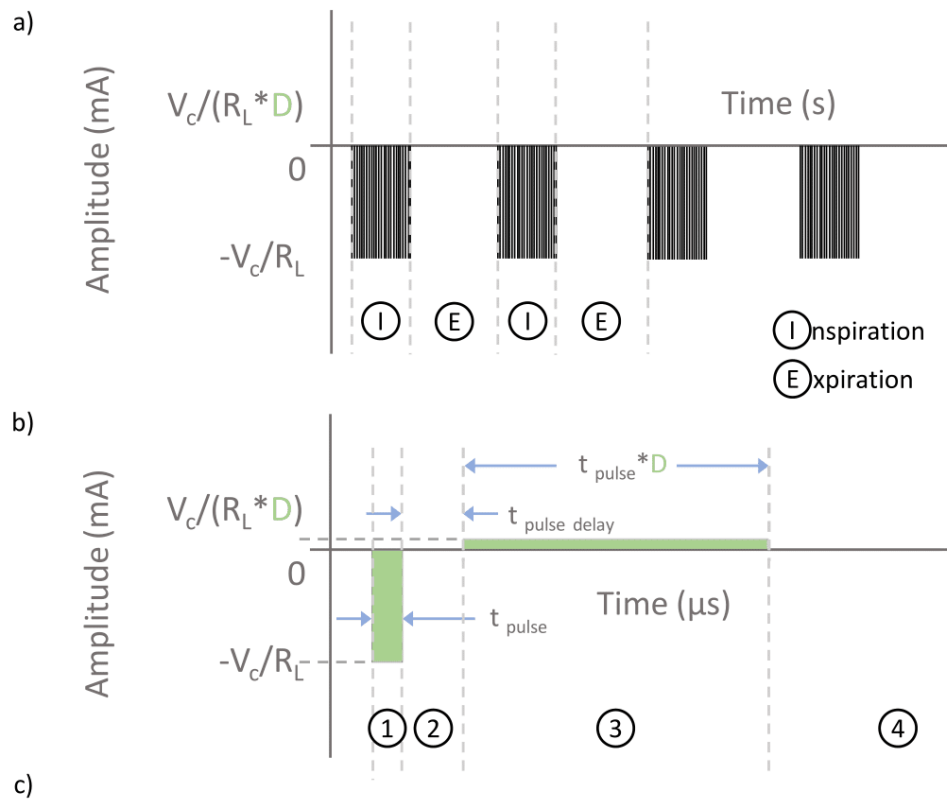


Figure 24: Signal Output: a) Breathing phases, b) Single pulse cycle, c) Logic control

Pulsing, as per requirements in Table 1, needs to happen at ~20Hz at maximum. Thus, a cycle of one negative and one positive pulse is repeating at a 50ms interval - “light years”, compared with the ~200 μ s simulation pulse width and a 16MHz clocking frequency available for STM8L152. Thus, initial iterations of the program had the device wake up right before each pulse cycle, control pulsing until the end of the positive recharge pulse, and go into a low power mode until the rest of the 50ms interval passes.

However, this is still not the most optimal solution to the problem. During wake-up and power-down times, microcontrollers usually waste more power than during stable modes, and having the microcontroller wake up multiple times during one operation cycle would not be very power-conscious.

The cyclical nature of the output signal is advantageous. First, there are a limited number of states that the MCU has to output - expiratory and inspiratory. Additionally, each pulse cycle within the inspiratory state has four distinct phases, shown in Figure 24.b. Because the pulse cycle is repeated many times for each breath, it is not strictly necessary to utilize the CPU for updating all of the peripherals at each pulse cycle phase - thus the MCU can be off for longer periods of time. Simply, peripheral registers need to be updated as per Figure 24.c.

A peripheral called Direct Memory Access (DMA) can be used to substitute the CPU in updating single registers of the pulsing peripherals. Peripherals can use DMA to access memory directly without involving the CPU. DMA read/write requests can be triggered by timer counters (among various other things), and can write single values from a software memory buffer into pre-specified peripheral registers.

With this technique, the device was pushed to its “configuration limits” by using various peripherals in conjunction with each other to output all three of the control signals without the need for CPU operation during pulsing - basically, “in hardware”. The detailed device software flow is described in detail in Appendix L, but general operation flow is described below.

At power-up, the CPU does some initial system configurations. When it directs the clock to the appropriate peripherals, they start operating and can be configured. The CPU then configures the pulsing peripherals and enables their outputs. The peripherals trigger each other in a timely manner and the three control signals start propagating through the hardware circuit. The CPU goes into a low-power mode for the rest of the inspiratory phase immediately after enabling these peripherals.

After the inspiratory phase is done (~1.1-1.3 seconds) and the peripherals go through multiple pulsing cycles, CPU is woken up by the Real Time Clock (RTC) counter overflow. Once stable, CPU immediately disables peripheral outputs (expiration phase thus begins), checks NFC memory for updates, re-configures the peripherals (including RTC) and software buffers based on the new information, and gates the peripherals (peripherals are off). Device goes into a “Halt” mode, in which everything shuts down except RTC, which keeps on ticking at 32.768kHz derived from the low-frequency external oscillator crystal. Thus, the CPU operation is kept short.

After the expiratory time is up, RTC counter overflows again, waking up the CPU. This time, all CPU does is enable the pulsing peripherals (which are now newly configured after last inspiratory time) and then it goes into sleep mode. Inspiratory phase begins and the process is repeated.

This particular order of operations accomplishes the following:

- 1) MCU-NFC Memory communication does not interfere with stimulation in any way. The NFC check and reconfiguration of pulsing peripherals is done *after* the inspiratory phase.
- 2) The stimulation is updated on a breath-to-breath basis - after the external transmitter writes to NFC memory, new values are used for stimulation at the very next breath cycle.
- 3) CPU is off for the overwhelming majority of the breath cycle (exact times still need to be estimated). It is power on briefly during the start of inspiratory and expiratory phases and only for computations that strictly require CPU function.
- 4) Because peripherals trigger each other in a pre-configured cascade, each of the four phases of the pulse cycle - simulation pulse, delay, recharge pulse, and the “off state” period - can be tightly controlled from the external transmitter.

2.6 Reliability Considerations

2.6.1 Failure Mode Chart

A failure modes chart containing possible mechanisms of failure, detection systems, and planned system responses of the device can be seen in Appendix M. We propose several features that should be implemented in future iterations of the project.

2.6.2 Multiple Processors

We propose a redundancy in microcontroller computing. The primary MCU would be similar in function to the MCU as programmed in the current prototype, and would be responsible for generation of stimulation signals. The secondary MCU would be monitoring the primary MCU's activity, and depending on irregularities it detects, would reset the primary MCU, set off alerts, place the primary MCU into a default life-sustaining mode, or even take over the primary MCU's functions.

2.6.3 Analog Error Detection

In order to make programming as simplistic as possible, and in general to increase reliability of checking systems, an analog error detection system may also be used. There are analog circuits that are capable of verifying that the signal's parameters fall within specific thresholds, and could take basic corrective actions if those boundaries are not met, which would indicate a problem in the system.

2.6.4 Backup Battery System

Although not yet implemented in the current iteration, it is recommended that a back-up non-rechargeable (more capacity, better reliability) battery be added to the design. This battery is to be used in the event of the rechargeable battery being depleted and to power speakers for alarms. As such, life sustaining function can be maintained by the device until the problem can be addressed

or until the patient can be switched over to mechanical ventilation. About a week of device function is planned.

2.6.5 Full System Redundancy

This system is designed to stimulate the two phrenic nerve branches separately with two electrically isolated systems, one for each side, similar to the way Avery's system has two separate receivers. As such, if one side fails, then the other should still be functional and can maintain life-sustaining function until the patient can be transferred to mechanical ventilation or the problem with the implant can be addressed. Optoisolating circuits could be used for synchronization.

2.6.6 Alert System

An alert system will be created to allow for the patient to be notified when there is an error with the implant or the external component.

2.6.6.1 Implant

- Level 1: Intermittent beep when charge needed + error code
 - Action Required: User needs to charge battery
- Level 2: More frequent beeps for any severe failures + error code
 - Action Required: User needs emergency room care, mechanical ventilator, or replacement device

2.6.6.2 External Component

- Messages based on read error codes
- Notifications to phone or other devices
- Flashing light and sound system

2.7 Testing

To demonstrate technical feasibility of the DAPhNe Stimulator, various tests were performed. Individual components were tested to verify they performed as theoretically planned, power consumption of sections of the circuit was tested, and an animal study protocol is in the process of being approved.

2.7.1 Power Consumption Testing

2.7.1.1 LTSpice Simulation

First, LTSpice was used to model the power consumption of the stimulation circuit alone. This was done by adding a very small resistor before the battery output, measuring the current across it over a period of time. The initial, non-steady state results were excluded, and then the average absolute value of current was found over about 0.1s, comprising nine full pulses. Data simulated over the entire 0.1s time period. In Figure 25 and Figure 26, green pulses indicate the current over the load; blue: current across the resistor in parallel with the battery.

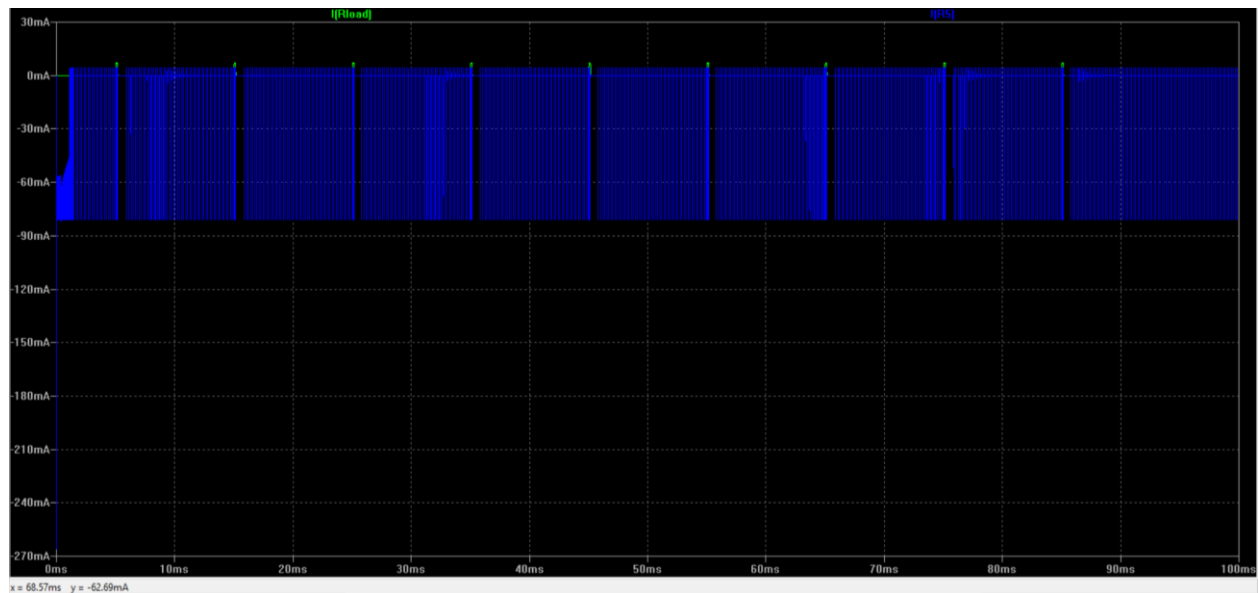


Figure 25: Simulation over a 0.1s time period

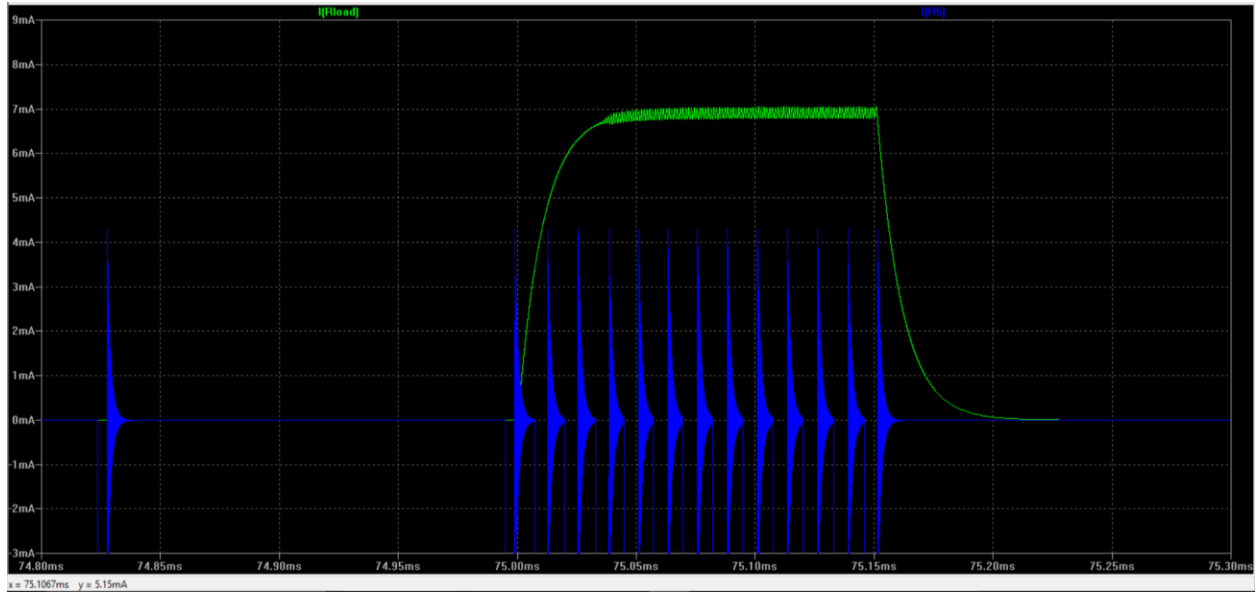


Figure 26: Simulation over a single pulse

The average current draw over the test resistor over 0.1s was about 2.3849mA, which means that powering the stimulation circuit alone would drain the LIR2450H battery after about 80 hours of function from a full charge.

2.7.1.2 Instantaneous Current Draw Testing

Once the PCB-based prototype was complete, power consumption testing was conducted using a benchtop voltage supply instead of a battery and by connecting an ammeter between the voltage source and the power rails (normally connected to the battery). It was set to 3.6V, to approximate normal function of the battery, and the instantaneous current draw of the circuit was recorded repeatedly. See Table 2 for ranges and maximum current draws obtained during testing.

Table 2: Instantaneous current draw per each section of the circuit with ranges and maximums.

	Range (mA)	Maximum (mA)
MCU (including LiPower)	2.5 - 10	10
Stimulation	4.5 - 5.5	5.5

The maximum draws were 10 mA and 5.5 mA of the MCU and stimulation sections of the circuit, respectively. Linearly adding these, and assuming the worst-case scenario that those maximum values are what the two boards draw constantly, the current battery from a full charge would last for about 12 hours.

2.7.1.3 Additional Considerations

Although that 12-hour value is less than would be necessary for convenient use (~18 hours), the current draw values obtained need a good deal of clarification. For one, the MCU is at its maximum power draw when its CPU is on, which only occurs for a couple of ms per cycle breath cycle. Also, this testing was conducted with three LED powered on. Each LED and corresponding current limiting resistor draw about 2-3 mA each, increasing the power draw of this prototype significantly. Finally, none of the components in this prototype are of medical quality or truly optimized for efficiency, which almost certainly would extend battery life, especially if the battery capacity were higher. It is known that significantly higher capacity batteries do exist that still could fit in an implant.

2.7.2 Device Output

Device output signal of 5mA amplitude was collected. Figure 27 shows the output of the first breakout board prototype acquired with nScope. Figure 28 shows the output of the second prototype – a much cleaner signal, although the polarity switching stage was not utilized.

The signal was programmed to be of 5mA amplitude, with a delay of twice the pulse duration (which was 200 μ s), and the amplitude ratio of the two signals was 10. Both signals met the specifications, but one can note that in the first prototype signal, there is an artifact on the recharge pulse due to the polarity switching circuit.

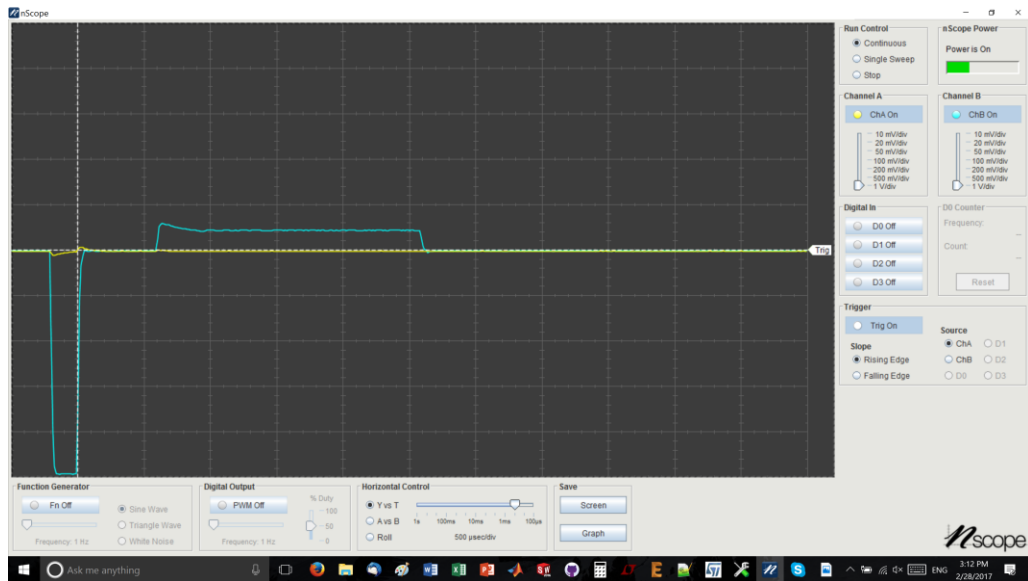


Figure 27: Output Signal: First Prototype

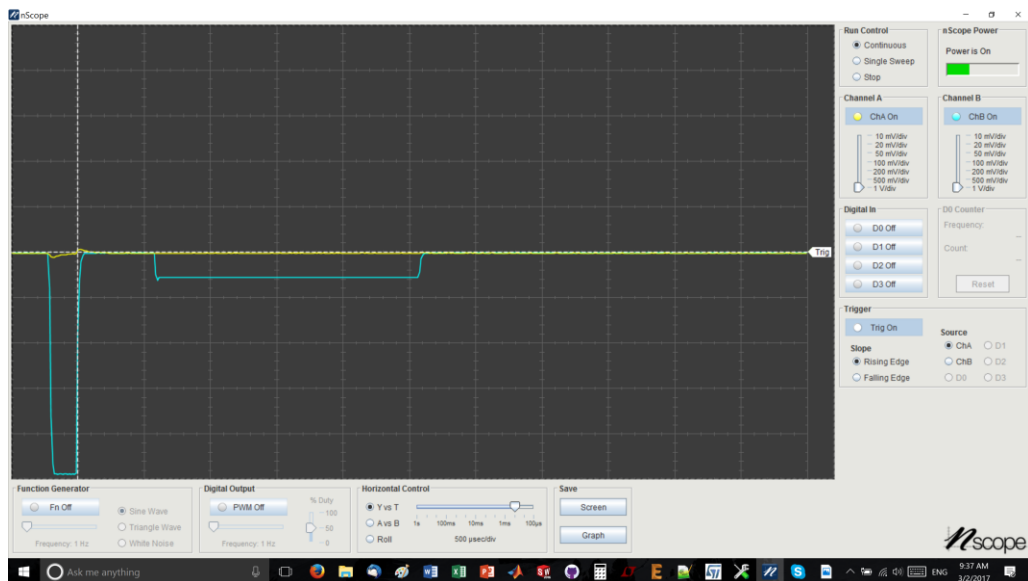


Figure 28: Output Signal: Second Prototype

2.7.3 Animal Testing

(Section not available in this version of the document)

2.7.2.1 *Specific Aims*

(Section not available in this version of the document)

2.7.2.2 Experimental Procedure

(Not available in this version of the document)

(Section not available in this version of the document)

(Section not available in this version of the document)

(Section not available in this version of the document)

3 External Device Development

3.1 User Interface Development

3.1.1 User Interface Interviews

To determine the user needs for the user interface of the external component of the device, interviews with parents of patients with CCHS and the clinical team at CAMP were conducted. Of the three parent interviews conducted, all 3 kids are 24/7 ventilator dependent and are on their Avery pacers during the day and the mechanical ventilator at night. The kids had a range of ages - 2.5, 6, and 9 years old, which provided a range of experience with the pacers and information on school aged kids as well as those not yet in school. The clinical team at CAMP have extensive experience working with these devices and the patients and demonstrated concerns with the lack of alarm systems, sturdiness of the device, and ability to secure settings. See Appendix P for the interview questions.

Three main user needs were defined from the interviews:

- 1) Accuracy of Controls: The parents strongly dislike the dials on the Avery system and want to better understand what the parameters are set to as well as have more accurate control over breathing rate should they need to adjust it. The clinicians said it is difficult to set the parameters and secure the dials.
- 2) Versatility of System: The parents want to have more settings than just the current active and quiet modes and also want the ability to easily switch between settings. Two of the parents said that having 3 settings would be life changing and the other parent said that 5 settings would be ideal.

- 3) Alarms: The Avery device does not have alarms if it malfunctions or indications that the battery level is low. The parents and clinicians would want to have a sound and an alert screen on the external device to notify them of any problems.

See Appendix Q for the detailed interview responses.

3.1.2 User Interface Design

From the interviews of parents of children with CCHS and clinicians, user needs were determined. A prototype of the user interface for the external component of the device was then designed for both the patient and doctor views.

On every screen, there are two bars at the top. The first is the status bar that shows the external transmitter battery level on the left, the implant battery level on the right, and the status of the left and right implants in the middle. The second bar shows the current pacing setting.

3.1.2.1 Lock Screen

The lock screen, seen in Figure 31.a shows the estimated battery time remaining for both the external component and the implant. A passcode will be required to open the device.

3.1.2.2 Home Screen

Once the user (patient or doctor) enters their passcode, the home screen will appear, Figure 31.b. This will have an option for checking system status, changing the breathing setting, viewing an activity log, and switching preferences. Additionally, there is a bottom bar on every screen to switch to emergency default mode, go back to the home screen, and view a notifications tab.

3.1.2.3 Check System Status

The check system status screen, Figure 31.c, will allow the user to view the implant battery level, estimated battery time remaining for both the implant and external component, as well as check the pacing status of the left and right implants.

3.1.2.4 Change Settings

The change settings screen, seen in Figure 31.d, shows all breathing settings that have been customized for that patient. To switch the setting, the user can tap on the setting they want to switch to and then confirm the switch.

3.1.2.5 View Setting Parameters – Patient View

If the patient wants to view the breathing parameters for a specific setting, they can tap the view button next to the setting of interest. The view setting parameters screen, Figure 31.e, shows the settings for breathing rate, inspiration time, pulse width, pulse amplitude, and pulse frequency.

3.1.2.6 View Activity Log

The view activity log screen, Figure 31.f, logs what setting was used and at what time.

3.1.2.7 Preferences Screen

The preferences screen, Figure 31.g, allows the user to adjust the display brightness, volume, and text size, as well as change their passcode.

3.1.2.8 Notifications Screen

The notification screen, Figure 31.h, displays notifications about battery level, connection status, or when settings have been switched.

3.1.2.9 View AND Change Setting Parameters – Doctor View

The doctor view will have the same screens as the patient view. The only difference is that the doctor will be able to adjust the breathing parameters for each setting to customize the settings to each individual patient. The doctor can increase or decrease the breathing rate, inspiration time, pulse width, pulse amplitude, and pulse frequency with the arrows next to each parameter. This will allow the doctor to have precise controls over the breathing settings. The screen to adjust the breathing parameters can be seen in Figure 31.i.

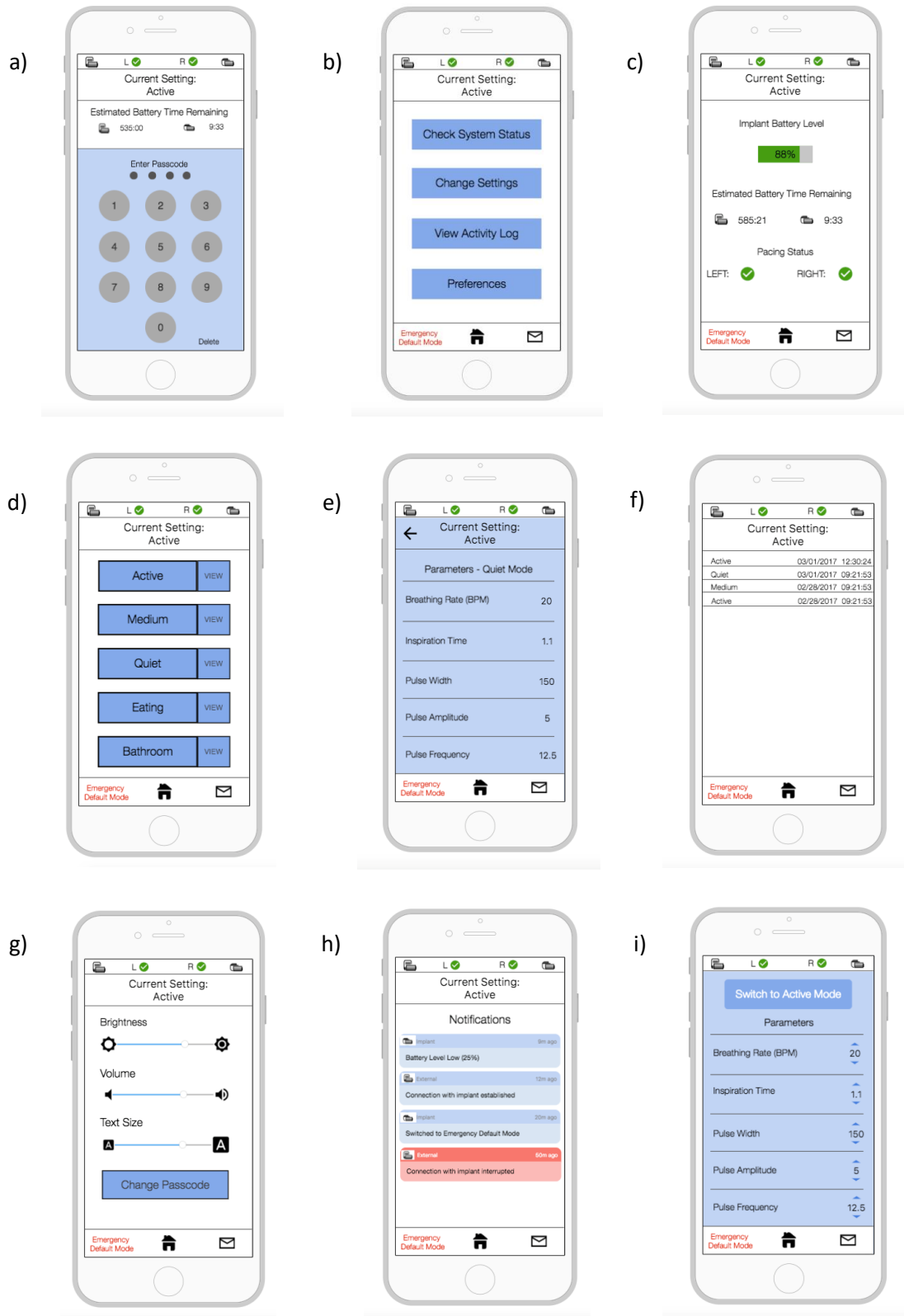


Figure 31: User Interface Screens

4 Next Steps

4.1 Power Consumption Testing

Thus far, only instantaneous power draw data has been obtained. Current/power draw as a function of time should be observed. As well, LEDs should be removed for later testing, in order to get more accurate readings. Finally, the battery should be fully charged, and then allowed to run the circuit until the battery runs dry, as a true test of how long battery charges would last.

4.2 Animal Testing

(Section not available in this version of the document)

4.3 User Interface

The current user interface design will be tested by interviewing parents of children with CCHS and clinical staff. This will inform the team of any changes that need to be made to the design.

4.4 Next Generation Prototype

Future iterations of prototypes will need to address the issues discovered with polarity switching, either through circuit or programming modifications. Other improvements might include better components, such as the battery or ICs for better reliability/tolerances or other specifications. PCBs may be redesigned for more even more miniaturization and to more closely approximate what the true device might appear to be like. A single PCB may unify both designs. Future iterations will also need to be compatible with Avery electrodes, which has not yet been addressed.

With these improvements, the next generation DAPhNe Stimulator will be the next step in improving the quality of life of children with CCHS.